

ARTICLE

DOI: 10.1038/s41467-017-01796-7

OPEN

Cooperative polariton dynamics in feedback-coupled cavities

Bimu Yao^{1,2}, Y.S. Gui¹, J.W. Rao¹, S. Kaur¹, X.S. Chen², W. Lu², Y. Xiao³, H. Guo⁴, K.-P. Marzlin^{5,6} & C.-M. Hu¹

The emerging field of cavity spintronics utilizes the cavity magnon polariton (CMP) induced by magnon Rabi oscillations. In contrast to a single-spin quantum system, such a cooperative spin dynamics in the linear regime is governed by the classical physics of harmonic oscillators. It makes the magnon Rabi frequency independent of the photon Fock state occupation, and thereby restricts the quantum application of CMP. Here we show that a feedback cavity architecture breaks the harmonic-oscillator restriction. By increasing the feedback photon number, we observe an increase in the Rabi frequency, accompanied with the evolution of CMP to a cavity magnon triplet and a cavity magnon quintuplet. We present a theory that explains these features. Our results reveal the physics of cooperative polariton dynamics in feedback-coupled cavities, and open up new avenues for exploiting the light-matter interactions.

¹Department of Physics and Astronomy, University of Manitoba, Winnipeg, Manitoba, Canada R3T 2N2. ²State Key Laboratory of Infrared Physics, Chinese Academy of Sciences, Shanghai 200083, China. ³College of Science, Nanjing University of Aeronautics and Astronautics, Nanjing, 210016, China.

⁴Department of Physics, McGill University, Montréal, Québec, Canada H3A 2T8. ⁵Department of Physics, St. Francis Xavier University, Antigonish, Nova Scotia, Canada B2G 2W5. ⁶Department of Physics and Atmospheric Science, Dalhousie University, Halifax, Nova Scotia, Canada B3H 4R2. Correspondence and requests for materials should be addressed to W.L. (email: luwei@mail.sitp.ac.cn) or to C.-M.H. (email: hu@physics.umanitoba.ca)

Controlling cooperativity is essential for utilizing the light-matter interactions¹. For light coupled with quantum systems, cooperativity measures the ratio of Rabi frequency to decay rates and can be controlled by changing the photon Fock state occupation². Recently, high cooperativity was demonstrated in hybridizing magnons and cavity microwave photons^{3–10}. In contrast to a single spin system², the harmonic oscillator nature of the ensemble of spins in the linear dynamic regime makes the magnon Rabi frequency independent of the photon number^{11–14}. Breaking the harmonic limit has been a pursuit of continuing interest in the study of collective dynamics, as, for example, in the case of the Kohn theorem^{15–17}. The same quest is developing in the new field of cavity spintronics¹⁸, where it is required for quantum control of collective spin dynamics^{19, 20}.

Here we show that a feedback cavity architecture breaks the harmonic limit for magnon-photon coupling. By increasing the voltage-controlled feedback photon number, we observe an increase of the Rabi frequency, accompanied with the evolution of the cavity magnon polariton^{7, 11, 12} to a cavity magnon triplet and a cavity magnon quintuplet. The unprecedented capability of on-chip control of magnon-photon cooperativity, which our theory links to the physics of cooperative polariton dynamics, may open up exciting opportunities for exploiting the light-matter interactions.

Results

Device architecture. Our experimental setup is schematically shown in Fig. 1a. We use a planar passive cavity (P) with a mode frequency ω_c to couple photons with the magnons (M) in a ferromagnetic insulator yttrium iron garnet (YIG). The YIG sphere is placed on top of the cavity at an adjustable distance d . An external magnetic field \mathbf{H} is applied parallel to the cavity to tune the magnon frequency ω_r . When ω_r approaches ω_c , the magnon-photon coupling²¹ produces the cavity magnon polariton (CMP)⁷ in the P-M device, which is detected by using a two-port vector network analyzer (VNA) that measures the transmission coefficient $S_{21}(\omega)$ of the P-cavity. The key innovation of our experiment, in comparison with the recent pioneering studies of magnon-photon coupling^{3–10}, is the design and implementation of an active cavity (A), which contains a microwave amplifier with voltage (V)-controlled gain (G_n). The two cavities (A and P) are carefully designed to have the same mode frequency. They are weakly coupled and phase matched to each other (see Supplementary Notes 1–3 for details). Such a feedback-coupled cavity architecture is crucial as it offers more capabilities than the versatile double beam technique²²: Essentially, the A-cavity acts as a feedback loop to compensate the microwave loss of the P-cavity, and produces a gain up to 360,000; the cavity quality factor is tunable up to 81,500, about three orders of magnitude higher than conventional planar cavities. Furthermore, feedback photons couple with the CMP, and thus coherently enhance the strong coupling in the P-M device. Altogether, these capabilities reveal a hidden cooperative effect of polariton dynamics, which has

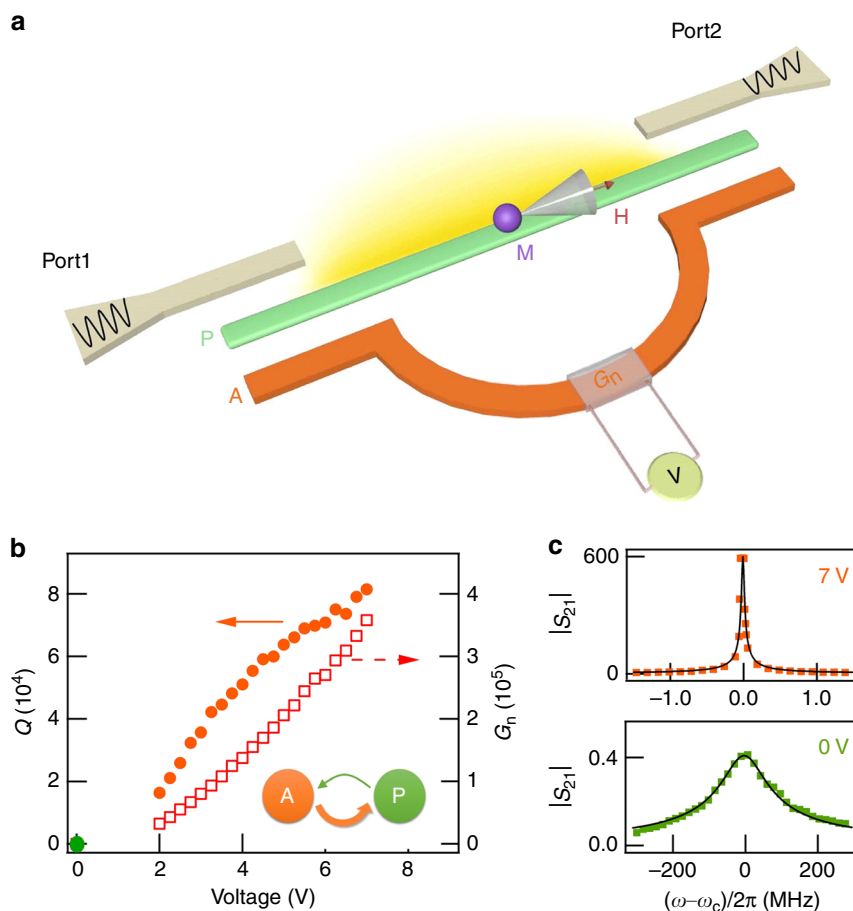


Fig. 1 Device architecture. **a** The A-P-M device consists of a passive cavity (P), an active cavity **A** with a voltage tuneable gain (G_n), and an YIG sphere with magnons (M). **b** The Q-factor and G_n of the A-P cavity circuit are tunable up to 81,500 and 360,000, respectively, by changing V. **c**, $|S_{21}|$ spectra of the cavity mode measured at $V = 0$ and 7 V, together with a fitted theoretical curve

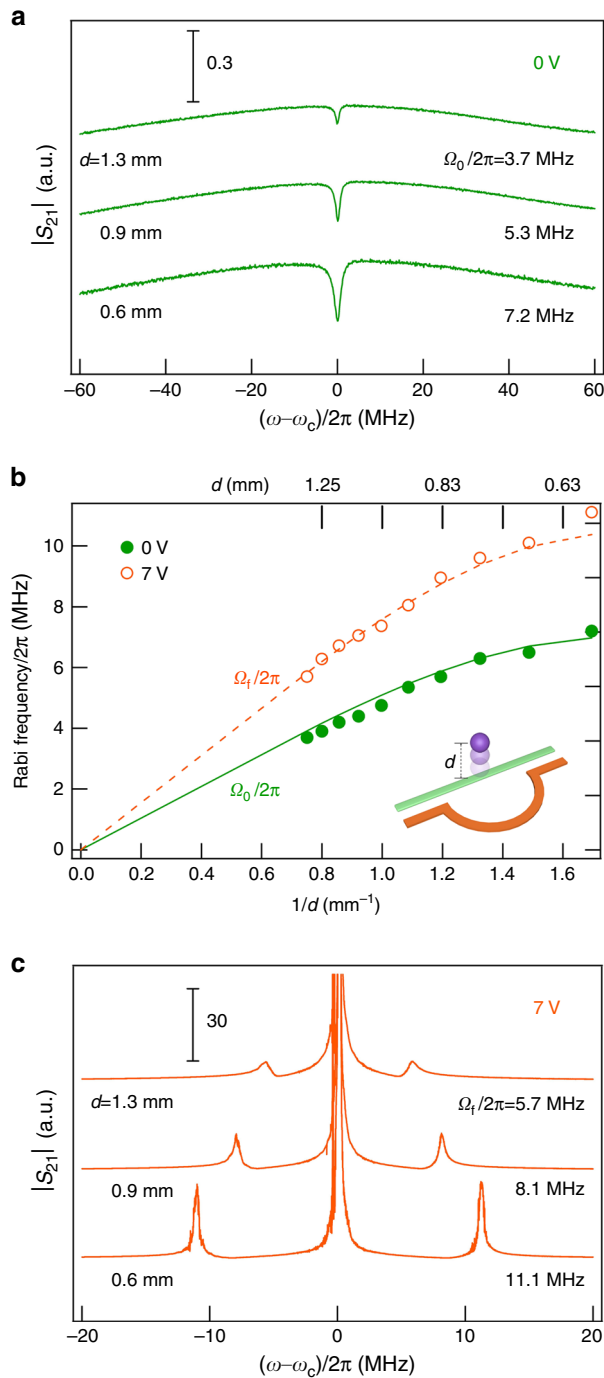


Fig. 2 Distance dependent Rabi frequency. **a** $|S_{21}|$ spectra measured at $\Delta = 0$ and $V = 0$ V, for $d = 1.3, 0.9,$ and 0.6 mm. The corresponding Rabi frequencies Ω_0 are determined by line shape fitting. **b** Rabi frequency as a function of d . The solid (open) circles represent data measured at $V = 0$ V (7 V). The solid curve represents $\Omega_0/2\pi$ calculated from Eq. (1) by using η determined from a Maxwell's equations solver, where the dashed curve is calculated with $\Omega_1 = 1.5\Omega_0$. **c** $|S_{21}|$ spectra measured at $\Delta = 0$ and $V = 7$ V. The Rabi frequencies Ω_f are determined from the mode splitting

escaped studies ever since 1954, when Dicke elucidated the cooperative molecular dynamics²³ that led to the development of super-radiant devices^{24, 25}.

A dozen A-P-M devices with different geometries were designed and showed consistent results, with a variety of new effects involving the light-matter interactions being revealed. In

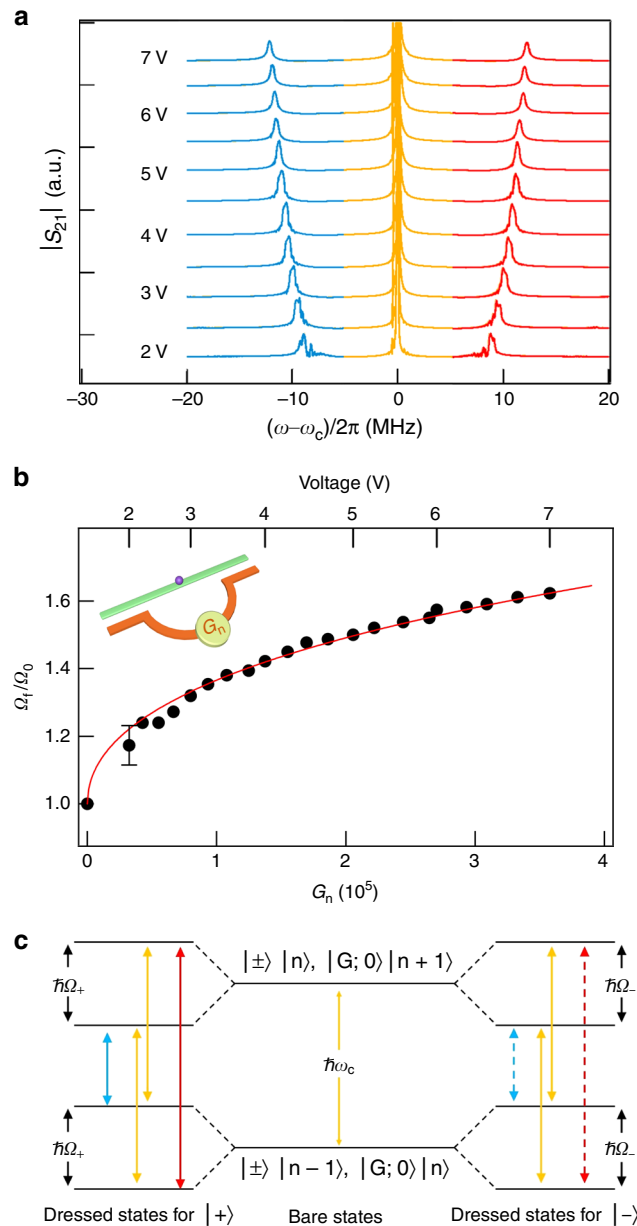


Fig. 3 Voltage dependent Rabi frequency. **a** $|S_{21}|$ spectra measured at $\Delta = 0$ and $d = 0.58$ mm ($\Omega_0/2\pi = 7.5$ MHz), for a series of V . **b** The measured (circles) and calculated (curve) ratio of Rabi frequencies Ω_f/Ω_0 plotted as a function of V and G_n . The error bar is the maximum uncertainty caused by the error when fitting the Rabi frequency. **c** Schematic dressed states of both CMP modes. At $\Delta = 0$, they produce the Mollow triplet with $\Omega_+ = \Omega_-$. At $\Delta \neq 0$, they produce the magnon quintuplet with $\Omega_+ \neq \Omega_-$. The detuning between the bare states is not shown for brevity

this paper the emphasis is on data rendered from a typical device, which focuses on the fundamental issue of the breaking of the harmonic protection of magnon-photon cooperativity.

The magnon mode we study has Gilbert damping parameter $\alpha = 2.0 \times 10^{-4}$, and the dispersion follows the Kittel formula $\omega_r = \gamma\mu_0(|H| + H_A)$. Here, $\gamma = 173$ GHz T⁻¹ is the electron gyromagnetic ratio, $\mu_0 H_A = 8.56$ mT is the effective field³⁻¹⁰, and μ_0 is the permeability of vacuum. We study the A-P-M devices by using three methods to systematically control the CMP: (i) tuning d to control the P-M coupling strength, (ii) tuning V to control the feedback photon number, and (iii) tuning H to change the frequency detuning $\Delta \equiv \omega_r - \omega_c$.

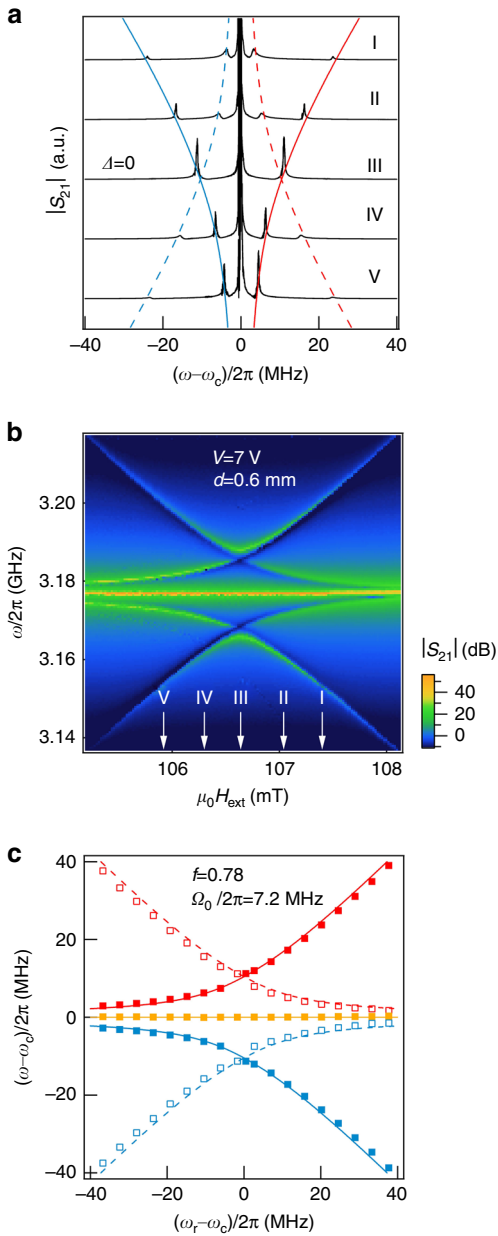


Fig. 4 Magnetic field dependent measurement. **a** $|S_{21}|$ spectra measured at $d = 0.6$ mm ($\Omega_0/2\pi = 7.2$ MHz) and $V = 7$ V ($f = 0.78$), for five different H fields as marked in **b**. The dispersion of the measured magnon quintuplet is plotted as a function of **b**, the magnetic field H , and **c**, the detuning $\Delta/2\pi$. The curves in **c** are calculated by using eq. (3)

Distance d dependent Rabi frequency. We begin our study with the feedback switched off ($V = 0$) and with an intra-cavity photon number of about 10^6 . Figure 2a shows the $|S_{21}|$ spectra measured at zero detuning ($\Delta = 0$). Within the broad cavity mode of $Q = 25$, a dip appears at $\omega_c/2\pi = 3.160$ GHz. This is the characteristic spectral response of CMP in the regime of magnetically induced transparency⁵ defined by $1/2Q > \Omega_0/\omega_c > \alpha$. The Rabi frequency Ω_0 depends on d since the rf field of the P-cavity increases with decreasing d . By fitting the $|S_{21}|$ spectra using the CMP theory^{5, 11, 12}, we deduce Ω_0 and plot the Ω_0 - d dependence in Fig. 2b (the solid circles).

The expected value of Ω_0 is given by^{3-5, 12, 21}

$$\Omega_0 = g_0 \sqrt{N}, \quad (1)$$

where $g_0 = \eta\gamma\sqrt{5\mu_0\hbar\omega_c/4V_c}$ is the vacuum Rabi frequency of a single spin, $N = 1.1 \times 10^{19}$ is the total number of spins in the YIG sphere, and V_c is the cavity mode volume. $\eta = h(d)/h(0)$ describes d -dependent spatial overlap between the rf field h and the magnon mode in YIG⁵, which we calculate by using a Maxwell's equations solver. With $V_c = 7.98 \times 10^{-5}$ m³ as the only fitting parameter, the calculated Rabi frequency is plotted in Fig. 2b (solid curve), and agrees well with the measured result.

Eq. (1) shows that Ω_0 has an \sqrt{N} -fold enhancement from g_0 . It is this cooperative spin dynamic effect^{14, 21, 23, 26} that makes cavity magnon systems highly interesting³⁻¹⁰. However, such a collective dynamics has a drawback: a single quantum two-level system can be saturated by one photon excitation, so that adding photons enhances the Rabi frequency², but the magnon-photon coupling exhibits classical behavior⁷ of coupled harmonic oscillators^{11, 12}. In the linear dynamic regime where the number of CMP $m \ll N$, the spin ensemble is far from being saturated, so that adding photons may increase m but does not change Ω_0 . Hence, in contrast to quantum systems², the magnon-photon cooperativity, $C \equiv 2(\Omega_0/\omega_c)^2 Q/\alpha$, has been found to be independent of photon number⁷. Breaking such a harmonic limit without interfering with the complex nonlinear magnetization dynamics^{21, 27, 28} seems impossible. But, as we reveal below, a distinct cooperative polariton dynamics may be used in the linear dynamic regime ($m \ll N$), which enables tuning of the magnon Rabi frequency by the changing of the feedback photon numbers.

Feedback dependent Rabi frequency. Figure 2c shows the $|S_{21}|$ spectra still measured at $\Delta = 0$, but with the amplifier switched on at $V = 7$ V. Feedback gain of $G_n = 3.6 \times 10^5$ with a feedback photon number of $n = 1 \times 10^{13}$ is created. The cavity mode frequency shifts slightly to $\omega_c/2\pi = 3.177$ GHz, while the Q -factor is significantly increased to 81,500. Noticeably, the A-P-M device enters the strong coupling regime³⁻¹⁰, where $\Omega_f/\omega_c > \alpha > 1/2Q$. Here, Ω_f is the Rabi frequency enhanced by the feedback photons, and is deduced from the two side peaks at $\omega_c \pm \Omega_f$. As shown in Fig. 2b, both Ω_f and Ω_0 increase with decreasing d , but the ratio of $\Omega_f/\Omega_0 = 1.5$ stays constant. Another remarkable feature is that a sharp resonance appears in the spectral center at ω_c , indicating that the twin CMP evolve to a cavity magnon triplet. It resembles the Mollow triplet²⁹, a canonical signature of the light-matter interaction observed in single quantum systems²².

The characteristic trait of the Mollow triplet is that the Rabi splitting increases with the photon number^{22, 29}. This is verified in Fig. 3a where we plot the $|S_{21}|$ spectra measured by changing V , while keeping the A-P-M device at $\Delta = 0$ with fixed $d = 0.58$ mm (corresponding to $\Omega_0/2\pi = 7.5$ MHz). As the feedback photon number is increased by increasing G_n , the Rabi splitting increases as shown in Fig. 3b. We find that, numerically, the measured Rabi splitting scales with G_n via a simple relation of $\Omega_f/\Omega_0 = (1 + \xi\sqrt{G_n})^{1/2}$ with $\xi = 2.7 \times 10^{-3}$. We also find that the scaling parameter ξ differs from device to device.

Cooperative polariton dynamics. Now, we quantitatively explain all these results through a model which we develop to unveil the underlying physics of cooperative polariton dynamics.

Without feedback coupling, the Hamiltonian describing N spins collectively coupled with a cavity mode is²⁶ $\hat{H}_0/\hbar = \omega_c \hat{p}^\dagger \hat{p} + \omega_r \hat{S}^z + g_0 (\hat{S}^+ \hat{p} + \hat{p}^\dagger \hat{S}^-)$. Here, the creation (annihilation) operators \hat{p}^\dagger (\hat{p}) describe the P-cavity mode, $\vec{S} = \sum_{j=1}^N \vec{S}_j$ is the collective spin (magnon) variable, with each spin in YIG characterized by the operators $\hat{S}_j^\pm = \hat{S}_j^x \pm i\hat{S}_j^y$ and \hat{S}_j^z .

Denoting $|(S, M)\rangle$ as the eigenstate of \hat{S}^2 and \hat{S}^z , and $|0\rangle$ as the vacuum of the radiation field, the ground state of the coupled

spin-photon system²¹ is $|G; 0\rangle = |(N/2, -N/2); 0\rangle$. The excited states, denoted by $|G; 1\rangle = |(N/2, -N/2); 1\rangle$ and $|E; 0\rangle = |(N/2, -N/2 + 1); 0\rangle$, respectively, are coupled to produce two CMP states $|\pm\rangle = c_{\pm}|E; 0\rangle \pm c_{\mp}|G; 1\rangle$, where $c_{\pm} = \sqrt{(\Omega_{\pm} \Delta/2)/2\Omega}$ are the state amplitudes with $\Omega \equiv \sqrt{\Omega_0^2 + (\Delta/2)^2}$. In the CMP basis, collective excitations from $|G; 0\rangle$ to $|\pm\rangle$ lead to the twin CMP modes appearing at $\omega_{\pm} = \omega_c + \Delta/2 \pm \Omega$.

With feedback coupling, all m CMPs produced by magnon-photon coupling are interacting collectively with n feedback photons. We find that such a cooperative polariton dynamics is described by the Hamiltonian (see Supplementary Notes 4–6 for details)

$$\hat{H}/\hbar = \omega_c \hat{a}^\dagger \hat{a} + \sum_{k=\pm} \omega_k \hat{m}_k^z + \sum_{k=\pm} \frac{c_k \Omega_0}{\sqrt{m}} (\hat{m}_k^+ \hat{a} + \hat{a}^\dagger \hat{m}_k^-), \quad (2)$$

where $\hat{a}^\dagger(\hat{a})$ describe the feedback photons, $\hat{m}_{\pm}^z = |\pm\rangle\langle\pm|$, $\hat{m}_{\pm}^+ = |\pm\rangle\langle G; 0|$, and $\hat{m}_{\pm}^- = |G; 0\rangle\langle\pm|$ are two-level operators written in the CMP basis.

Eq. (2) links two coherent cooperative dynamics: the collective excitation of the N spin ensemble by magnon-photon coupling, and the collective de-excitation of the m CMP ensemble due to the coupling of polaritons with the coherently feedback photons. It leads to dressed states², as shown in Fig. 3c. The feedback enhanced Rabi frequency is calculated (see Supplementary Note 6) for each CMP mode by considering the coupling between the states $|\pm\rangle|n\rangle$ and $|G; 0\rangle|n+1\rangle$, and we find

$$\Omega_{\pm} = \sqrt{(\Omega_{\pm} \Delta/2)^2 + 2(f\Omega_0)^2(\Omega_{\pm} \Delta/2)/\Omega}, \quad (3)$$

where $f \equiv \sqrt{n/m}$ is the feedback factor that can be tuned by changing G_n .

At $\Delta = 0$, we obtain from Eq. (3) $\Omega_{\pm} = \Omega_f = \Omega_0 \sqrt{1 + 2f^2}$, which means that the two sets of dressed states shown in Fig. 3c have the same Rabi splitting. Therefore, they produce the same triplet at ω_c and $\omega_c \pm \Omega_f$, as observed in Figs. 2c and 3a. Setting $f = 0.78$ for $V = 7$ V, we obtain $\Omega_f = 1.5\Omega_0$, which produces the dashed line in Fig. 2b.

When the gain is tuned by changing V , we have $n \propto G_n$. In the linear regime, by assuming that the number of CMP is proportional to the non-equilibrium magnetization which depends linearly on the rf field h ²⁷, we find $m \propto \sqrt{G_n}$. Hence, Eq. (3) leads to the scaling of $\Omega_f/\Omega_0 = (1 + \xi\sqrt{G_n})^{1/2}$ at $\Delta = 0$, where ξ is a device-specific parameter. This gives the theoretical curve calculated in Fig. 3b.

Furthermore, Eq. (3) predicts that at $\Delta \neq 0$, a cavity magnon triplet will split because $\Omega_+ \neq \Omega_-$. Five modes are expected to appear at ω_c , $\omega_c \pm \Omega_+$, and $\omega_c \pm \Omega_-$. Indeed, such an intriguing cavity magnon quintuplet, produced by the cooperative dynamics of CMP, occurs when we change the H field.

Cavity magnon quintuplet. Figure 4a shows the $|S_{21}|$ spectra measured at different H , with fixed $V = 7$ V and $d = 0.6$ mm. Clearly, when Δ is tuned away from zero, each of the modes at $\omega_{\pm}/2\pi = 3.177 \pm \Omega_f/2\pi$ split into a doublet, and the splitting increases with $|\Delta|$. The quintuplet dispersions are plotted in Fig. 4b, 4c as a function of H and Δ , respectively. Using $f = 0.78$ and $\Omega_0/2\pi = 7.2$ MHz determined from Fig. 2, we calculate the dispersions from Eq. (3) without any other parameters. The result agrees very well with the measured data, as shown in Fig. 4c.

Thus, the A-P-M devices coherently utilize two correlated aspects of cooperative dynamics in the feedback-coupled cavity systems. The first aspect, known for more than six decades as cooperative spin dynamics, is rooted in Dicke's seminal work²³.

Signified by the Dicke factor \sqrt{N} , it describes the collective dynamics of the N spin system coupled with the vacuum of the radiation field. The second aspect, revealed in this work as cooperative polariton dynamics, shows the collective dynamics of m polaritons coupled with the higher Fock states of n feedback photons, which manifests itself by the feedback factor of $\sqrt{n/m}$. Using this effect, we demonstrate the breaking of harmonic protection for magnon-photon cooperativity in the linear dynamic regime ($m \ll N$), and discover the evolution of CMP to a cavity magnon triplet and a quintuplet. We note that although our experiment is based on a ferromagnetic YIG sample, the physics of cooperative polariton dynamics revealed in our study is general. With the feedback cavity technique, new avenues are in sight for harnessing the light-matter interactions at room temperature in the development of cavity spintronics and quantum technologies.

Methods

Experimental details. The planar microwave cavities are fabricated from Rogers RT/duroid 5880 High Frequency Laminates. The relative permittivity of the substrate is 2.2, with a loss tangent of 0.0009. The substrate is 1.57 mm thick and covered by 17.5 μ m thick copper layers on both sides. An YIG sphere (M) with a diameter of 1 mm is attached to a Polytetrafluoroethylene rod which is transparent to microwaves. The rod is further connected to a stepping motor, so that the position of YIG sphere can be precisely controlled to tune the coupling strength between the YIG sphere and the cavity. All the measurements are performed at room-temperature. The cavity along with the YIG sphere as a whole hybrid system is immersed in a static external magnetic field. The S_{21} spectra of the hybrid system is obtained using a Vector Network Analyzer (Agilent PNA N5230C) to measure the transmission signal of the cavity from port 1 to 2 with an input microwave power of -50 dBm.

Theoretical description. The measured S_{21} spectra of the A-P and P-M devices are analyzed by using input-output theory to determine the quality factor, gain, and coupling strength. The measured dispersions of the A-P-M hybrid system are quantitatively and consistently explained by developing a model based on quantum theory. Without feedback photons, N spins are collectively driven by the radiation field of the P-cavity mode. When the gain of the A-cavity is switched on, in addition to the magnon-photon coupling that produces m CMPs, the ensemble of CMP also collectively couples with the n coherently feedback photons. These two coherently linked cooperative dynamics are described by Eq. (2) in the main text, as well as by Supplementary Eq. 10. Based on this Hamiltonian, the quintuplet dispersions and the feedback photon enhanced Rabi frequency are calculated. In the Supplementary Notes 4–6, the theoretical derivation and the quantum picture of both magnon-photon coupling and polariton-photon coupling are explained in detail.

Data availability. All relevant data are available from the authors.

Received: 26 April 2017 Accepted: 16 October 2017

Published online: 10 November 2017

References

1. Haroche, S. Controlling photons in a box and exploring the quantum to classical boundary. *Rev. Mod. Phys.* **85**, 1083 (2013).
2. Cohen-Tannoudji, C., Dupont-Roc, J. & Grynberg, G. *Atom-Photon Interactions* (Wiley-VCH, 2004).
3. Huebl, H. et al. High cooperativity in coupled microwave resonator ferrimagnetic insulator hybrids. *Phys. Rev. Lett.* **111**, 127003 (2013).
4. Tabuchi, Y. et al. Hybridizing ferromagnetic magnons and microwave photons in the quantum limit. *Phys. Rev. Lett.* **113**, 083603 (2014).
5. Zhang, X., Zou, C. L., Jiang, L. & Tang, H. X. Strongly coupled magnons and cavity microwave photons. *Phys. Rev. Lett.* **113**, 156401 (2014).
6. Goryachev, M. et al. High-cooperativity cavity QED with magnons at microwave frequencies. *Phys. Rev. Appl.* **2**, 054002 (2014).
7. Bai, L. et al. Spin pumping in electro-dynamically coupled magnon-photon systems. *Phys. Rev. Lett.* **114**, 227201 (2015).
8. Haigh, J. A., Lambert, N. J., Doherty, A. C. & Ferguson, A. J. Dispersive readout of ferromagnetic resonance for strongly coupled magnons and microwave photons. *Phys. Rev. B* **91**, 104410 (2015).

9. Tabuchi, Y. et al. Coherent coupling between a ferromagnetic magnon and a superconducting qubit. *Science* **349**, 405 (2015).
10. Wang, Y.-P. et al. Magnon Kerr effect in a strongly coupled cavity-magnon system. *Phys. Rev. B* **94**, 224410 (2016).
11. Yao, B. M. et al. Theory and experiment on cavity magnon-polariton in the one-dimensional configuration. *Phys. Rev. B* **92**, 184407 (2015).
12. Harder, M., Bai, L., Match, C., Sirker, J. & Hu, C.-M. Study of the cavity-magnon-polariton transmission line shape. *Sci. China Phys. Mech. Astronomy* **59**, 117511 (2016).
13. Cao, Y., Yan, P., Huebl, H., Goennenwein, S. T. & Bauer, G. E. Exchange magnon-polaritons in microwave cavities. *Phys. Rev. B* **91**, 094423 (2015).
14. Chiorescu, I., Groll, N., Bertaina, S., Mori, T. & Miyashita, S. Magnetic strong coupling in a spin-photon system and transition to classical regime. *Phys. Rev. B* **82**, 024413 (2010).
15. Kohn, W. Cyclotron resonance and de Haas-van Alphen oscillations of an interacting electron gas. *Phys. Rev.* **123**, 1242 (1961).
16. Hu, C. M., Batke, E., Köhler, K. & Ganser, P. Interaction coupled cyclotron transitions of two-dimensional electron systems in GaAs at high temperatures. *Phys. Rev. Lett.* **75**, 918 (1995).
17. Maag, T. et al. Coherent cyclotron motion beyond Kohn's theorem. *Nat. Phys.* **12**, 119 (2016).
18. Hu, C.-M. Dawn of cavity spintronics. *Phys. Canada* **72**, 76 (2016).
19. Tabuchi, Y. et al. Quantum magnonics: the magnon meets the superconducting qubit. *Comp. R. Phys.* **17**, 729 (2016).
20. Zhang, X., Zou, C. L., Jiang, L. & Tang, H. X. Cavity magnomechanics. *Sci. Adv.* **2**, e1501286 (2016).
21. Soykal, Ö. O. & Flatté, M. E. Strong field interactions between a nanomagnet and a photonic cavity. *Phys. Rev. Lett.* **104**, 077202 (2010).
22. Xu, X. et al. Coherent optical spectroscopy of a strongly driven quantum dot. *Science* **317**, 929 (2007).
23. Dicke, R. H. Coherence in spontaneous radiation processes. *Phys. Rev.* **93**, 99 (1954).
24. Scheibner, M. et al. Superradiance of quantum dots. *Nat. Phys.* **3**, 106 (2007).
25. Noe, G. T. II et al. Giant superfluorescent bursts from a semiconductor magneto-plasma. *Nat. Phys.* **8**, 219 (2012).
26. Agarwal, G. S. Vacuum-field Rabi splittings in microwave absorption by Rydberg atoms in a cavity. *Phys. Rev. Lett.* **53**, 1732 (1984).
27. Gui, Y. S., Wirthmann, A., Mecking, N. & Hu, C.-M. Direct measurement of nonlinear ferromagnetic damping via the intrinsic foldover effect. *Phys. Rev. B* **80**, 060402 (2009).
28. Wang, Y.-P., Zhang, D., Li, T.-F., Hu, C.-M., & You, J. Q. Bistability of Cavity Magnon-Polaritons. Preprint at <http://arxiv.org/abs/1707.06509v1> (2017).
29. Mollow, B. R. Power spectrum of light scattered by two-level systems. *Phys. Rev.* **188**, 1969 (1969).

Acknowledgements

This work was funded by NSERC and NSFC (11429401) grants (C.M.H.). We thank B.W. Southern, G.C. Tabisz, G. Bridges, and X.L. Gao for discussions. We would also like to acknowledge CMC Microsystems for providing equipments that facilitated this research.

Author contributions

B.M.Y. and Y.S.G. fabricated the devices, conducted the experiment and analyzed the data. B.M.Y. prepared all figures and wrote the Methods section. J.W.R. and S.K. contributed to the device design and data analysis, respectively. W.L. and X.S.C. provided support and conceptual advice. Y.X. and C.M.H., in discussions with H.G. and K.-P.M., developed the theory. C.-M.H. supervised the project, interpreted the results, and wrote the manuscript. All authors discussed the results and commented on the manuscript.

Additional information

Supplementary Information accompanies this paper at doi:10.1038/s41467-017-01796-7.

Competing interests: The authors declare no competing financial interests.

Reprints and permission information is available online at <http://npg.nature.com/reprintsandpermissions/>

Publisher's note: Springer Nature remains neutral with regard to jurisdictional claims in published maps and institutional affiliations.



Open Access This article is licensed under a Creative Commons Attribution 4.0 International License, which permits use, sharing, adaptation, distribution and reproduction in any medium or format, as long as you give appropriate credit to the original author(s) and the source, provide a link to the Creative Commons license, and indicate if changes were made. The images or other third party material in this article are included in the article's Creative Commons license, unless indicated otherwise in a credit line to the material. If material is not included in the article's Creative Commons license and your intended use is not permitted by statutory regulation or exceeds the permitted use, you will need to obtain permission directly from the copyright holder. To view a copy of this license, visit <http://creativecommons.org/licenses/by/4.0/>.

© The Author(s) 2017